Journal of Pharmaceutical Sciences

Sulphonylurea Structure-Pharmacokinetic Relationships in the Pancreas and Liver

Journal:	*Journal of Pharmaceutical Sciences*
Manuscript ID:	08-342
Wiley - Manuscript type:	Research Article
Date Submitted by the Author:	06-Jun-2008
Complete List of Authors:	Fanning, Kent; University of Queensland, Medicine Anissimov, Yuri; Griffith University, School of Biomolecular and Physical Sciences roberts, michael; Univ Qld, Medicine
Keywords:	Log P, Passive diffusion/transport, Pharmacokinetics, Permeability, Structure-transport relationship, Distribution

Sulphonylurea Structure-Pharmacokinetic Relationships in the Pancreas and Liver

Kent J Fanning[1,2], Yuri G Anissimov[1,3] and Michael S Roberts[1]

[1] Therapeutics Research Unit, Department of Medicine, Princess Alexandra Hospital, University of Queensland, Woolloongabba, Queensland, Australia
[2] To whom correspondence should be addressed. (phone: 61 7 3406 8606. fax: 61 7 3240 5806. email: kent.fanning@dpi.qld.gov.au)
[3] School of Biomolecular and Physical Sciences, Griffith University, Queensland, Australia

Abstract

This study examined the structure-pharmacokinetic relationships for the sulphonylureas in the perfused rat pancreas and liver. Multiple indicator dilution studies were conducted with bolus injections of tolbutamide, chlorpropamide, gliclazide, glipizide, glibenclamide and glimepiride, and a reference marker albumin, in the perfused pancreas and liver. Individual solute pharmacokinetics were analysed using nonparametric moment analysis and non linear regression assuming a physiologically based pharmacokinetic model. All solutes had similar shaped outflow concentration-time profiles in both the pancreas and liver, but varied in extraction. Negligible drug extraction was evident in the pancreas. Hepatic extraction ranged from 0.03 (tolbutamide) to 0.52 (glibenclamide) and could be related to solute lipophilicity and perfusate protein binding. The sulphonylurea mean transit times in both the pancreas and liver varied 4 and 9 fold respectively and were related to the lipophilicity and perfusate protein binding of the drug. The permeability surface area product of sulphonylureas from the perfusate into the organs were greater in the liver and were mainly determined by lipophilicity (pancreas, $r^2 = 0.89$; liver, $r^2 = 0.80$). The distribution of the sulphonylureas in both the perfused pancreas and perfused liver was dependent on their lipophilicity and perfusate protein binding.

Introduction

The pancreas and liver are often considered together in defining the effectiveness of antidiabetic drugs.[1] The pancreas is an essential organ that consists of two functionally distinct parts - the exocrine and endocrine pancreas. Pathologies of the pancreas include diabetes mellitus, pancreatitis and pancreatic cancer. We have recently established a single pass perfused pancreas model and used the multiple indicator dilution technique to examine the distribution of reference markers and tolbutamide.[2] Single pass in situ or isolated perfused liver systems have also been used to define solute structure-pharmacokinetic relationships for barbiturates,[3] phenolic compounds,[4] and cationic drugs.[5] Transport in the liver can occur by passive diffusion, active transport by various transporters (eg., organic anion-transporting polypeptide, fatty acid binding protein, see review article for details[6]) and by endocytosis.[7] At this time, the main solute physicochemical determinants of passive hepatic transport are lipophilicity [4,5,8] and pKa.[5] Many of these studies have used the multiple indicator dilution technique pioneered in the dog in vivo by Goresky.[9]

Sulphonylureas (SUs) are widely used to treat type 2 diabetes mellitus. Whilst it is known that SUs bind to receptors on the pancreatic cell membrane and enter endocrine tissue, little is known about drug distribution kinetics in the pancreas. The SUs are of interest for several key reasons; they are one of the major drug classes used in treating type 2 diabetes mellitus by acting on the pancreas, they undergo extensive metabolism in the liver and may mediate an action by binding to the liver and there is a range of physicochemical properties within the drug class, particularly in regard to lipophilicity (see Table I). Furthermore, there is interest in understanding the pharmacokinetics of these compounds in both the pancreas and liver in regards to

elucidating their transport mechanism(s)[10,11] and their distribution in the pancreas,[12] liver[13] and whole body.[10] We are not aware of any study that has investigated the relationship between solute physicohemical properties and their distribution in the perfused pancreas.

In this work, we investigated the relationship between the physicochemical properties of the SUs and their pharmacokinetics in the pancreas and liver. Our studies involved single pass indicator dilution experiments in the perfused rat pancreas and liver and analysis of the resulting outflow profiles with a physiologically based pharmacokinetic model.

Materials and Methods

Chemicals

Tolbutamide, chlorpropamide, glipizide, gliclazide and glibenclamide were all purchased from Sigma-Aldrich (St. Loius, MO). Glimepiride was kindly donated by Aventis Pharma (Frankfurt, Germany). [^{3}H]-water, [^{14}C]-sucrose and [^{125}I]-albumin were obtained from Perkin Elmer (Melbourne, Australia).

In situ Rat Pancreas Perfusions

Male Wistar rats weighing 190-250 g were fed a commercial diet and water ad libitum. All procedures involving the animals were carried out with adherence to the University of Queensland Animal Care Committee guidelines (AEC#MED/249/05/UQ). The pancreas perfusions were carried out similarly to those described previously.[2] Briefly, following overnight fasting, animals were anaesthetized by interperitoneal injection of 80 mg/kg ketamine (Parnell Laboratories, Sydney, Australia) and 10 mg/kg xylazine (Bayer, Sydney, Australia). Laparotomy was performed and heparin (300 units) injected into the inferior vena cava to prevent clotting. The pancreas was perfused via the coeliac and superior mesenteric trunks of the aorta, using a 22 G cannula, with 2% bovine serum albumin (BSA), 4% dextran, 3-[N-Morpholino]propane-sulphonic acid (MOPS) buffer, at a pH of 7.4, and effluent was collected from the portal vein. The perfusion medium was heated to 37°C and oxygenated using an artificial lung consisting of silastic tubing. Immediately following the commencement of perfusion the animal was killed by thoracotomy. The viability of the preparation was assessed by macroscopic appearance, oxygen consumption and perfusion pressure.

Portions of pancreas were collected following the end of each perfusion to ascertain drug tissue levels. The pancreas tissue was minced with scissors, prior to the addition of acetonitrile, then homogenized and left for 24 hours before being processed and analysed by high performance liquid chromatography (HPLC).

In situ Rat Liver Perfusions

Male Wistar rats weighing 215-285 g were fed a commercial diet and water ad libitum. All procedures involving the animals were carried out with adherence to the University of Queensland Animal Care Committee guidelines (AEC#MED/249/05/UQ). The liver perfusions were carried out similarly to that previously described.[5] Briefly, following overnight fasting, animals were anaesthetized by interperitoneal injection of 80 mg/kg ketamine (Parnell Laboratories, Sydney, Australia) and 10 mg/kg xylazine (Bayer, Sydney, Australia). Laparotomy was performed and heparin (300 units) injected into the inferior vena cava to prevent clotting. The liver was perfused via the portal vein, using a 16 G cannula, with 2% BSA MOPS buffer containing 15% (v/v) prewashed canine red blood cells (RBCs), at a pH of 7.4. The perfusion medium was heated to 37°C and oxygenated using an artificial lung consisting of silastic tubing. Immediately following the commencement of perfusion, the animal was killed by thoracotomy. The viability of the preparation was assessed by macroscopic appearance, oxygen consumption, bile flow and perfusion pressure.

Bolus Studies

Pancreas perfusions were conducted at 2 ml/min. Following an equilibration phase of 15 min, a series of 5 individual 20µl bolus injections were undertaken. These

consisted of any 4 of the 6 sulphonylureas (tolbutamide, chlorpropamide, gliclazide, glipizide, glibenclamide, glimepiride), all at 200 µg/ml in a random order, [^{125}I]-albumin, [^{14}C]-sucrose and [^{3}H]-water. Samples from the outflow catheter were collected by a fraction collector over 6.5 min (15 x 2s, 4 x 4s, 5 x 7s, 3 x 14s, 3 x 28s, 5 x 36s). Injections were given every 10 min, with the total perfusion time approximately 65 min.

Liver perfusions were conducted at 15 ml/min. Following an equilibration phase of 15 min, a series of 7 individual 50µl bolus injections were undertaken. These consisted of the 6 sulphonylureas (tolbutamide, chlorpropamide, gliclazide, glipizide, glibenclamide, glimepiride), all at 1 mg/ml, in a random order, together with [^{125}I]-albumin, and [^{14}C]-sucrose and [^{3}H]-water. Samples from the outflow catheter were collected by a fraction collector over 4 min (20 x 1s, 5 x 4s, 5 x 10s, 5 x 30s). Injections were given every 10 min, with the total perfusion time approximately 75 min.

Analytical Procedure

Samples from both liver and pancreas perfusions were analysed using a Tri-Carb 2700TR (Packard, Meriden, CT) scintillation counter to determine the levels of [^{14}C]-sucrose and [^{3}H]-water, as previously described [2,5]. The concentration of [^{125}I]-albumin was determined by using a Cobra 2 gamma counter (Packard, Meriden, USA) and corrected as necessary for radioactive decay over time. The injection mixture was diluted 1:50 in the perfusion medium prior to counting by the same procedure as the perfusate samples.

HPLC Instrumentation

The HPLC system consisted of a SCL-10A XL auto injector (Shimadzu), SCL-10A VP system controller (Shimadzu), LC-10AT liquid chromatograph (Shimadzu) and a SPD-10AV UV-VIS detector (Shimadzu). 10 – 50 µl of each sample was injected onto a C_{18} column (Waters Symmetry) with a mobile phase of (a) 40 % acetonitrile/60% water (for tolbutamide,[2] chlorpropamide and glipizide) or (b) 50% acetonitrile/50% water (for glicliazide, glibenclamide, glimepiride). The pH of the mobile phase was adjusted to 3 with concentrated phosphoric acid in both cases, then vacuum filtered and degassed prior to use. The mobile phase was pumped at 1 ml/min and detection undertaken at 230nm.

Extraction Procedure

Samples and standards were prepared similarly for analysis by HPLC. For all compounds, 100 µl of acetonitrile and 50 µl of internal standard were added to 100 µl of sample. The solution was briefly vortexed and then centrifuged at 10000 rpm for 5 min. Internal standards were made up as 2.5 µg/ml solutions in acetonitrile. Tolbutamide was the internal standard for chlorpropamide and glipizide, chlorpropamide was the internal standard for tolbutamide,[2] gliclazide was the internal standard for glibenclamide and glimepiride, and glibenclamide was used as the internal standard for gliclazide.

Calibration and Assay Validation

Calibration standards were linear between 0 and 20 µg/ml, with r^2 values of >0.995. The within-day coefficient of variation was measured by setting up and running three separate standard curves on the same day. Three unknown samples were also run. The

mean of each unknown was determined using the separate curves. The standard deviation of the means was divided by the overall mean. The coefficient of variation ranged from 1.5 to 3.3 %. The limit of detection was determined by injecting diluted calibration standards and was found to be 0.01 µg/ml for tolbutamide, 0.05 µg/ml for chlorpropamide, 0.025 µg/ml for glipizide, 0.05 µg/ml for gliclazide, 0.01 µg/ml for glibenclamide, and 0.025 µg/ml for glimepiride.

Perfusion Medium Binding

The fraction of drug that was unbound in the perfusate, f_{uB}, was determined for each sulphonylurea. 10 µg/ml solutions were made up in 2% BSA MOPS buffer, with or without 15% (v/v) prewashed canine RBCs at pH 7.4, and incubated at 37°C for 30 min. One ml of each solution was loaded into a Centrifree ultracentrifugation device (Amicon, YM-30) and centrifuged at 1100xg for 5 min. The collected filtrate and the incubation solution were then extracted as described for the perfusion samples and similarly analysed by HPLC. The fraction unbound was determined as the concentration of drug in the filtrate divided by the concentration in the incubation solution.

Data Analysis

The raw radioactive counts for albumin and HPLC concentrations for the drugs were converted to outflow fraction per ml after first subtracting corresponding background concentrations. To describe albumin outflow after bolus injection, the data for both liver and pancreas were modelled using the function:

$$C_B(t) = \frac{1}{Q} L^{-1}\left\{ \hat{f}_{cath}(s)\hat{f}_B(s) \right\} \quad (1)$$

where Q is the flow rate and $\hat{f}_i(s)$ is an empirical function defined in Laplace domain as

$$\hat{f}_i(s) = p\exp\left\{\frac{1}{CV_1^2} - \left[\frac{2MT_1}{CV_1^2}\left(s + \frac{1}{2MT_1 CV_1^2}\right)\right]^{1/2}\right\} + (1-p)\exp\left\{\frac{1}{CV_2^2} - \left[\frac{2MT_2}{CV_2^2}\left(s + \frac{1}{2MT_2 CV_2^2}\right)\right]^{1/2}\right\} \quad (2)$$

[14] where MT_1, MT_2, CV_1^2, CV_2^2 and p are all empirical parameters, estimated by nonlinear regressions. The catheter effect function $\hat{f}_{cath}(s)$ (i=cath in equation 2) was estimated first by nonlinear regression of the catheter [^{125}I]-albumin outflow-time profile using equation (2) and a weighting of $1/y^2$. The catheter parameters were then fixed ($p = 0.312$, $MT_{1cath} = 4.35$ sec, $MT_{2cath} = 11.11$ sec, $CV_{1cath}^2 = 0.04$, $CV_{2cath}^2 = 0.48$ for the pancreas catheter and $p = 0.421$, $MT_{1cath} = 1.27$ sec, $MT_{2cath} = 1.88$ sec, $CV_{1cath}^2 = 0.12$, $CV_{2cath}^2 = 0.87$ for the liver catheter) and parameters for the pancreas/liver obtained by fitting data with equation (1). The pharmacokinetic parameters for individual SUs were then defined by fitting data with a physiologically based pharmacokinetic model, defined by the function:

$$C_S(t) = \frac{1}{Q} L^{-1}\left\{\hat{f}_{cath}(s)\hat{f}_B\left[s + k_{in}\left(1 - \frac{k_{out}}{k_{out} + k_e + s}\right)\right]\right\} \quad (3)$$

[15] where $C_S(t)$ is the outflow concentration-time profile for the drug, L^{-1} is the inverse Laplace transform, k_{in} is the permeability rate constant from the vascular and interstitial space to the cellular space, k_{out} is the permeability rate constant from the tissue to the vascular and interstitial space defined by: $k_{out} = k_{in}.V_B/V_C$, and V_C and V_B are the cellular and extracellular spaces and k_e is the rate constant of drug elimination in the cellular space. The permeation clearance, from the perfusate to the

tissue, CL_{pT}, is defined as $k_{in} * V_B$, and is related to the fraction of solute unbound in the perfusate, f_{uB}, and the permeability surface area product (*PS)* by the equation $CL_{pT} = f_{uB} * PS$.[14] The intrinsic clearance from the liver, CL_{int} is defined as $k_e * V_C$.[5]

The recoveries (F), extraction ratio (E) and $MTTs$ of the solutes were estimated by statistical moments using the trapezoidal rule and appropriate corrections for the time period after the last sample:

$$F = \frac{Q\int_0^\infty Cdt}{Dose} = \frac{Q.AUC}{Dose} \quad (4)$$

$$E = 1 - F \quad (5)$$

And

$$MTT = \frac{\int_0^\infty tCdt}{\int_0^\infty Cdt} = \frac{AUMC}{AUC} \quad (6)$$

Statistical Analysis

Regression and multiple liver regression analyses were conducted using the software package SPSS (SPSS Inc., Chicago, USA). Barbiturate and other commonly used drugs,[8] phenolic compounds,[4] cationic drugs,[5] and SU data were used in the multiple liver regression analyses of the hepatic permeability surface area product versus solute physicochemical parameters for solute taken up into the liver by passive diffusion.

Results

The average weight of the pancreas preparations (n=5) was 1.88 ± 0.22 g. Several parameters indicated that the pancreas was viable during perfusion: perfusion pressure (43.0 ± 5.7 cm H_2O), dry/wet ratio (0.27 ± 0.02), oxygen consumption (0.38 ± 0.09 μmol·min^{-1}·g^{-1} of preparation) and pH of the outflow perfusate (7.17 ± 0.02 pH units) (2). The volumes occupied by albumin, sucrose and water, in the perfused pancreas, were 0.16 ± 0.03, 0.31 ± 0.05, and 0.76 ± 0.14 ml g^{-1} of tissue, respectively. Indices used to confirm liver perfusion viability (n=4), perfusion pressure (10.3 ± 1.3 cm H_2O), liver dry/wet ratio (0.29 ± 0.01), oxygen consumption (2.32 ± 0.41 μmol·min^{-1}·g^{-1} of liver), pH of the outflow perfusate (7.25 ± 0.03 pH units) and bile flow (0.81 ± 0.26 μl·min^{-1}·g^{-1} of liver) were consistent with a viable liver perfusion (5). The livers had an average weight of 7.81 ± 0.66 g. The volumes occupied by albumin, sucrose and water, in the perfused liver, were 0.27 ± 0.02, 0.31 ± 0.02 and 0.79 ± 0.14 ml g^{-1} liver, respectively. The estimated cellular volume, V_C, for the liver was 0.48 ± 0.11 ml g^{-1} liver.

Table I shows the f_{uB}, molecular weight, log P_{app} (log of the octanol:water partition coefficient at pH 7.4) and pKa for the SUs. The f_{uB} ranged from 0.005 ± 0.0002 (glibenclamide) to 0.225 ± 0.046 (gliclazide) and 0.005 ± 0.0001 (glibenclamide) to 0.181 ± 0.010 (gliclazide), for the RBC-free and RBC-containing perfusate, respectively. In both perfusates, log f_{uB} was inversely proportional to log P_{app}: RBC-free, log f_{uB} = -0.85 – 0.81 log P_{app} (r^2 = 0.97, p<0.001); RBC-containing, log f_{uB} = – 0.90 - 0.80 log P_{app} (r^2 = 0.90, p<0.005).

Figures 1 and 2 show the outflow concentration-time profiles for the SUs and albumin in the perfused rat pancreas and liver, respectively. In both the pancreas and liver,

glimepiride (1F and 2F) and glibenclamide (1E and 2E) had the shortest tail sections. Tolbutamide (1A and 2A) and chlorpropamide (1B and 2B) had intermediate tails, and gliclazide (1C and 2C) had the longest tail sections. Glipizide had a tail that was more pronounced in the liver (2D), than in the pancreas (1D). The nonparametric moments derived from data in Figures 1 and 2 are shown in Table II. Normalized variance (CV^2) for all SUs and reference compounds was significantly higher in the pancreas than in the liver. The extraction ratio (*E*) for SUs was negligible in the pancreas but varied more than 10 fold in the liver.

Also shown in Figures 1 and 2 are the nonlinear regressions of the outflow concentration time data assuming a physiologically based pharmacokinetic model (Fig 1G, 2G). The kinetic parameters derived from the model are summarised in Table III. Larger values for k_{in} were found in the liver, with the values for tolbutamide ($p<0.02$) and glibenclamide ($p<0.01$) being significantly higher. In contrast, k_{out} was generally larger in the pancreas than the liver and significantly larger for glibenclamide ($p<0.003$) and glipizide ($p<0.02$). The k_{in}/ k_{out} in the liver was significantly higher than in the pancreas for gliclazide ($p<0.04$), glipizide ($p<0.01$), and glimepiride ($p<0.03$), and approached significance for glibenclamide ($p=0.079$).

Also shown in Table III are the pharmacokinetic variables derived from the kinetic parameters. The values of CL_{pt} and *PS* were all significantly higher in the liver than in the pancreas for all SUs except for chlorpropamide and the *PS* of tolbutamide.

Figure 3 shows the relationships obtained between the statistical moments derived from each SU outflow concentration-time profile in the pancreas and liver and SU

physicochemical parameters. The specific relationships, for both organs, are between MTT and log P_{app} (A-pancreas, B-liver), and MTT and log f_{uB} (C-pancreas, D-liver). In the liver the following relationships are shown, CV^2 and log P_{app} (E), CV^2 and log f_{uB} (F), E and log P_{app} (G) and E and log f_{uB} (H). MTT was inversely related to log P_{app} for both the pancreas and liver but directly proportional to f_{uB} in the pancreas and liver. CV^2 was not significantly related to log P_{app} or log f_{uB} in the pancreas. CV^2 was inversely related to log P_{app} and log f_{uB} in the liver when glipizide (having the largest CV^2) was removed. Similarly, a relationship approaching statistical significance was seen between E and log P_{app} only when glipizide was excluded. In contrast E was inversely proportional to log f_{uB} based on all data.

In both the pancreas and liver k_{in} was directly proportional to log f_{uB} with the regression results being, $k_{in} = 0.05 \log f_{uB} + 0.15$ ($r^2 = 0.82$, $p<0.02$) and $k_{in} = 0.13 \log f_{uB} + 0.28$ ($r^2 = 0.76$, $p<0.03$), respectively.

Figure 4 shows the relationship in the pancreas between log CL_{pt} and log P_{app} (A), log CL_{pt} and log f_{uB} (B) and log PS and log P_{app} (C) and in the liver for log PS and log P_{app} (D). Regression analysis showed a direct relationship between log CL_{pt} and log P_{app} and log CL_{pt} and log f_{uB}. There was no apparent relationship between log CL_{pt} and log P_{app} or log CL_{pt} and log f_{uB} in the liver. The log PS was directly proportional to log P_{app} in both the pancreas and liver. There was no apparent relationship between the log of the intrinsic clearance (CL_{int}) and log P_{app} or log f_{uB}. When multiple regressions where undertaken, using log P_{app} and log f_{uB}, the percentage of data explained was increased for these derived parameters and the before mentioned

statistical moments. For example, the data for the pancreas yielded the following regressions,

$MTT = 6.11 \log P_{app} + 17.05 \log f_{uB} + 33.28$ ($r^2 = 0.94$).

$\log CL_{pt} = 0.02 \log P_{app} + 0.34 \log f_{uB} + 0.37$ ($r^2 = 0.95$).

$\log PS = -0.36 \log P_{app} - 1.08 \log f_{uB} + 0.03$ ($r^2 = 0.98$).

The values for *PS* and various physicochemical properties of solutes derived from liver perfusion studies are shown in Table IV. Lipophilicity was the main determinant for *PS* (Fig 5A), a physiologically based pharmacokinetic parameter that is independent of route of metabolism. However, the regression for *PS* was improved when either hydrogen bonding or polar surface area were included as covariates (Fig 5B). Molecular weight and melting point were not significant predictors for hepatic passive *PS* for various solutes.

Discussion

This study appears to be the first study to describe solute structure pharmacokinetic relationships in the perfused pancreas. The study used a series of SUs and the multiple indicator dilution technique in the single pass perfused rat pancreas. Also included in the study were injections of SUs into the liver and a comparison of the structure pharmacokinetic relationships in the pancreas and liver. The multiple indicator dilution technique used in this work involved the rapid injection of labelled albumin, sucrose and water as reference markers to the vascular, extracellular and total water spaces. In this study [^{125}I]-albumin was chosen as the vascular reference marker for SU pharmacokinetics because the SUs had high protein binding in the 2% BSA-containing perfusate.

Sucrose and water have been used as reference markers in perfused preparations of the pancreas[2] and liver.[5] Sucrose occupies the extracellular space and this is slightly larger than the albumin space in the liver.[16] Water is used to provide the total water volume, which when subtracted from the extracellular space yields the cellular volume. The sucrose and water volume in the perfused pancreas were similar to the corresponding volumes in the perfused liver.

The extraction of the solutes examined in this study was negligible in the pancreas but significant in the liver. Consistent with these results, tolbutamide has negligible extraction in the pancreas[2] but significant extraction in the liver.[17] In contrast, amino acids show significant extraction in both the perfused pancreas[18] and liver.[19]

Most studies on solute structure pharmacokinetic relationships in perfused organs have been in the liver. The classes of drugs studied include barbiturates,[3] phenolic compounds,[4] and cationic compounds.[5] To date there appears to be no data available on the distribution of solutes in the pancreas performed by the multiple indicator dilution technique. Hori et al showed that there was minimal extraction of several drugs in the pancreas when assessed using pancreatic biopsies in rabbits.[20]

This work has shown that in the pancreas, lipophilicity (log P_{app}) and plasma protein binding (f_{uB}) are major physicochemical determinants for SU disposition, explaining 94% of the linear regression for mean transit time (MTT), 95% for permeation clearance (log CL_{pt}) and 98% for the permeability surface-area product (log *PS*).

Solute CV^2 arises from a combination of vascular dispersion and tissue permeation and binding.[21] In the present work, a low CV^2 was found for the liver, consistent with its homogeneous vasculature and previous work.[22] The much greater CV^2 values in the pancreas perfusions are presumably due to the organ's heterogeneous vasculature [2]. In other heterogeneous perfusion preparations, such as the head, large CV^2 values for vascular dispersion have been shown, reflecting the different vascular beds.[23]

Permeation clearance is the ability of a compound to cross a cell wall and is usually expressed as *PS* for unbound drugs. This work has shown that *PS* for solutes in the pancreas is directly proportional to lipophilicity (as expressed by log P_{app}). Kamp et al (2003) suggested that glibenclamide had higher transport than tolbutamide across phospholipid bilayers due to differences in lipophilicity.[11]

Of particular interest in defining drug pancreas tissue levels from in vivo plasma concentrations is the tissue:plasma partition coefficient, $[C_{tissue}]/[C_{plasma}]$. This ratio for SUs can be estimated by the ratio k_{in}/ k_{out} for the pancreas as this study has showed SUs have negligible extraction in the pancreas. The partitioning characteristics of drugs have been previously investigated in the pancreas by whole animal injection.[20] Ouyang and Lien (1984) subsequently looked at these results and concluded that lipid solubility was the most important physicochemical property in determining this distribution.[24] We have reanalysed the data of Hori et al using log P_{app} as the physicochemical parameter representing lipophilicity and found that log $[C_{tissue}]/[C_{plasma}]$ = a log P_{app} + b. A similar relationship is predicted from the $[C_{tissue}]/[C_{plasma}]$ for SUs from this study as log k_{in}/ k_{out} = 0.13 log P_{app} + 0.55.

In our present study, glibenclamide and glimepiride had the smallest volume of distribution in the pancreas. Previous findings, using pancreatic islets, had reported that the volume of distribution of glibenclamide was much greater than the other SUs.[25] It is noted that the islets which constitute only 1-2 % of the mass of the pancreas do not represent the whole organ seen during perfusion and glimepiride and glibenclamide internalize into β-cells extensively.[26] Furthermore, these previous studies were conducted with protein-free media[25] and the uptake of the SUs into micro dissected islets has been shown to be significantly reduced by the addition of albumin to the culture medium.[27] The importance of protein binding as a determinant for SU uptake into the pancreas is also evident in a comparison of the results from this present work using tolbutamide with 2% BSA in the perfusate and our earlier work using tolbutamide with 0.5 % BSA in the perfusate.[2] The peak height of the outflow

profile of tolbutamide, in our pancreas perfusions, was 3.5 times higher and occurred 1.7 times earlier where 2% BSA was used in the perfusate.

This study also showed that the *E*, MTT and *PS* of the SUs in the liver were found to be related to solute lipophilicity. The range of *E*s found (0.03-0.52) put the SUs into the low clearance category,[28] where clearance depends mainly upon the solute f_{uB} and the CL_{int} and not on hepatic blood flow. The outflow profiles and low k_{out} parameter estimates for glipizide, glibenclamide and glimepiride suggest that, when taken up by the liver, these SUs are retained within the hepatocytes. Although SU receptor expression has not been observed in the liver, the SUs do bind to liver tissue.[29] The concentrations at which SUs are effective on hepatocytes was seen to differ greatly with a concentration of 70 nM observed for glibeclamide, 5 μM for glipizide and 100 μM for tolbutamide.[29] This may indicate differences in binding affinity of the SUs to the liver. Interestingly, non-specific microsomal binding has been best predicted by log P_{app} for acidic compounds.[30] This would suggest that glibenclamide and glimepiride would display the strongest binding in the liver which is evident from their small k_{out} values in the present study. Glipizide was an outlier in the regressions of CV^2 and *E* because of its low k_{out} relative to the other SUs with similar lipophilicities. As a consequence it appeared to be more trapped in the liver leading to increased CV^2 and *E*.

The membrane of the hepatocytes was more permeable to the SUs than the pancreas (as shown by larger values of k_{in} , CL_{pt} and *PS*). These higher values of drug influx in the liver appeared to offset the limiting effect that low f_{uB} has on SU hepatic extraction. The uptake of tolbutamide into the liver in this study ($0.19 \pm 0.04\ s^{-1}$) is similar to the

k_{in} of 0.211 ± 0.025 s^{-1} found for liver slices.[31] Worboys et al noted that more lipophilic compounds had slower uptake rates (k_{in}) but were more concentrated in the hepatocytes as was seen in this present study. Tolbutamide appears to have a larger uptake into liver slices than into isolated islets.[32]

The larger ratio of k_{in}/ k_{out} in the liver for gliclazide, glipizide, glibenclamide and glimepiride is presumably indicative of more binding in the liver than the pancreas. The difference can be attributed to a higher tissue protein concentration in the liver, 112.8 mg protein·g^{-1} liver,[33] than in the pancreas, 83.1 mg protein·g^{-1} protein (unpublished result from our laboratory) and the associated greater number of non-specific binding sites. Consistent with our findings, glibenclamide has been shown to have a greater partitioning into the liver than into the pancreas after intravenous injection.[34]

The use of tracer doses and a washout period between bolus doses, allowed any interference caused by previous SU injections, in a given experiment, to be minimized. There was no significant order of injection differences in the disposition kinetics of the individual SUs recognizing that the SUs were injected in a randomized order across the various replicates. Further, no SU concentration was found in the outflow perfusate (less than limit of detection) immediately prior to each injection. SUs are reported to undergo hepatic metabolism by carboxylation and hydroxylation.[35,36] This does not rule out that some drugs may have remained in the liver at the time of the next injection. For example, if no glibenclamide left the cell following the last collection point, the intracellular concentration of glibenclamide could be maximally

calculated to be 14 μM. This is larger than the reported IC_{50} of glibenclamide, 11 μM, to inhibit the metabolism of S-warfarin by human liver microsomes.[37]

It has been well established that the CL_{int} in the liver can vary between drug classes but within a given class, CL_{int} is often related to lipophilicity (as expressed by drug P_{app} eg., [5]). The main reason that CL_{int} is sometimes unrelated to physical structure and is not defined by physicochemical properties is because a specific drug-receptor configuration is necessary for metabolism and/or biliary excretion.[6] Validation of the present set of data is evident as the SUs have previously been defined to have a low first-pass metabolism.[35] In addition, CL_{int} obtained for tolbutamide in the present study, 0.059 ± 0.117 $ml \cdot min^{-1} \cdot g^{-1}$, is similar to that previously obtained by Schary and Rowland. In that study, a CL_{int} of 0.08-0.36 $ml \cdot min^{-1} \cdot g^{-1}$ was obtained after infusion studies in the perfused rat liver.[17] As CL_{int} is a determinant of *E* and MTT, generalized relationships with physicochemical properties for solutes from different classes are not possible without adjusting for the class effect. *PS* is independent of metabolism class.

PS, for the set of solutes examined here, defines passive transport across the hepatocellular membrane. Transporter-mediated uptake has been defined for many groups of compounds, with structure/transporter relationships being identified.[6] Previous workers have related liver *PS* due to passive diffusion with solute lipophilicity.[4,5,8] Figure 5a shows that the present results are consistent with these earlier results and that log P_{app} is a major determinant of *PS*. This regression was improved by also including solute polarity as a covariate. The percentage of data explained by the regression increased from 62 to 76 or 75 when the number of

hydrogen-bonding groups or polar surface area, respectively, were included as covariates. Figure 5b shows how there is a greater correlation between observed and predicted values of log *PS* when both log P_{app} and number of hydrogen-bonding groups are used in the regression (r^2=0.76) or log P_{app} and polar surface area (r^2=0.75), than when only log P_{app} is used (r^2=0.62). The parameters, number of hydrogen-bonding groups and polar surface area are highly correlated (r^2=0.89) indicating that the choice of the variable is an arbitrary consideration. The relationship between lipophilicity (directly proportional) and hydrogen bonding (inversely proportional) of compounds and their permeability appear to follow similar characteristics in the liver as to what is evidenced in gastrointestinal absorption and the blood brain barrier.[38] Supporting evidence includes the inverse relationship between log *PS* and polar surface area for human intestinal Caco-2 cells[39] and between log *PS* and Abraham descriptors related to hydrogen bonding for the blood brain barrier.[40] Molecular weight has only been found to be a major determinant in skin permeability[41] and was found not to improve the regressions for log *PS* versus log P_{app}, in the liver, when included as a covariate.

In conclusion, negligible extraction of the SUs was present in the pancreas whereas moderate extraction was present in the liver for glipizide, glibenclamide and glimepiride. Distribution in both the pancreas and liver was dependent on log P_{app} and f_{uB}.

Acknowledgements

This work was financially supported by a grant from the National Health and Medical Research Council of Australia and a University of Queensland Development grant.

We thank Julijana Nikolovski and Alexander Klentzos for assistance in the perfusions.

Abbreviations

BSA, bovine serum albumin; MOPS, 3-[N-Morpholino]propane-sulphonic acid; RBC, red blood cell; E, organ (pancreas/liver) extraction ratio; MTT, mean transit time; CV^2, normalized variance; HPLC, high performance liquid chromatography; MW, molecular weight; f_{uB}, fraction unbound in perfusate; log P_{app}, octanol:water partition coefficient at pH=7.4; CL_{pt}, permeation clearance; *PS*, permeability surface area product; CL_{int}, intrinsic clearance; $k_{in,}$ influx rate constant; k_{out}, efflux rate constant; k_e, elimination rate constant.

References

1. Baig NA, Herrine SK, Rubin R 2001. Liver disease and diabetes mellitus. Clin Lab Med 21(1):193-207.
2. Fanning KJ, Roberts MS 2007. Characterization of the Physiological Spaces and Distribution of Tolbutamide in the Perfused Rat Pancreas. Pharmaceutical Research 24(3):512-520.
3. Chou CH, Evans AM, Fornasini G, Rowland M 1993. Relationship between lipophilicity and hepatic dispersion and distribution for a homologous series of barbiturates in the isolated perfused in situ rat liver. Drug Metab Dispos 21(5):933-938.
4. Mellick GD, Roberts MS 1999. Structure-hepatic disposition relationships for phenolic compounds. Toxicol Appl Pharmacol 158(1):50-60.
5. Hung DY, Chang P, Weiss M, Roberts MS 2001. Structure-hepatic disposition relationships for cationic drugs in isolated perfused rat livers: transmembrane exchange and cytoplasmic binding process. J Pharmacol Exp Ther 297(2):780-789.
6. Mizuno N, Niwa T, Yotsumoto Y, Sugiyama Y 2003. Impact of drug transporter studies on drug discovery and development. Pharmacol Rev 55(3):425-461.
7. Goresky CA 1980. Uptake in the liver: the nature of the process. Int Rev Physiol 21:65-101.
8. Chou C, McLachlan AJ, Rowland M 1995. Membrane permeability and lipophilicity in the isolated perfused rat liver: 5-ethyl barbituric acid and other compounds. J Pharmacol Exp Ther 275(2):933-940.
9. Goresky CA 1963. A linear method for determining liver sinusoidal and extravascular volumes. Am J Physiol 204:626-640.
10. Boileau P, Wolfrum C, Shih DQ, Yang TA, Wolkoff AW, Stoffel M 2002. Decreased glibenclamide uptake in hepatocytes of hepatocyte nuclear factor-1 alpha-deficient mice - A mechanism for hypersensitivity to sulfonylurea therapy in patients with maturity-onset diabetes of the young, type 3 (MODY3). Diabetes 51:S343-S348.
11. Kamp F, Kizilbash N, Corkey BE, Berggren PO, Hamilton JA 2003. Sulfonylureas rapidly cross phospholipid bilayer membranes by a free-diffusion mechanism. Diabetes 52(10):2526-2531.
12. Geng X, Li L, Watkins S, Robbins PD, Drain P 2003. The insulin secretory granule is the major site of K(ATP) channels of the endocrine pancreas. Diabetes 52(3):767-776.
13. Petzinger E, Fuckel D 1992. Evidence for a Saturable, Energy-Dependent and Carrier-Mediated Uptake of Oral Antidiabetics into Rat Hepatocytes. Eur J Pharmacol 213(3):381-391.
14. Weiss M, Roberts MS 1996. Tissue distribution kinetics as determinant of transit time dispersion of drugs in organs: application of a stochastic model to the rat hindlimb. J Pharmacokinet Biopharm 24(2):173-196.
15. Weiss M, Kuhlmann O, Hung DY, Roberts MS 2000. Cytoplasmic binding and disposition kinetics of diclofenac in the isolated perfused rat liver. Br J Pharmacol 130(6):1331-1338.
16. Hung DY, Chang P, Cheung K, Winterford C, Roberts MS 2002. Quantitative evaluation of altered hepatic spaces and membrane transport in fibrotic rat liver. Hepatology 36(5):1180-1189.

17. Schary WL, Rowland M 1983. Protein binding and hepatic clearance: studies with tolbutamide, a drug of low intrinsic clearance, in the isolated perfused rat liver preparation. J Pharmacokinet Biopharm 11(3):225-243.
18. Munoz M, Sweiry JH, Mann GE 1995. Insulin stimulates cationic amino acid transport activity in the isolated perfused rat pancreas. Exp Physiol 80:745-753.
19. Holecek M, Rysava R, Safranek R, Kadlcikova J, Sprongl L 2003. Acute effects of decreased glutamine supply on protein and amino acid metabolism in hepatic tissue: A study using isolated perfused rat liver. Metabolism 52(8):1062-1067.
20. Hori R, Arakawa M, Okumura K 1978. Tissue distribution and metabolism of drugs. II. Accumulation and permeation of drugs in the rabbit pancreas. Chem Pharm Bull 26(4):1135-1140.
21. Roberts MS, Fraser S, Wagner A, McLeod L 1990. Residence Time Distributions of Solutes in the Perfused-Rat-Liver Using a Dispersion Model of Hepatic Elimination .1. Effect of Changes in Perfusate Flow and Albumin Concentration on Sucrose and Taurocholate. J Pharmacokinet Biopharm 18(3):209-234.
22. Weiss M, Ballinger LN, Roberts MS 1998. Kinetic analysis of vascular marker distribution in perfused rat livers after regeneration following partial hepatectomy. J Hepatol 29(3):476-481.
23. Foster KA, Mellick GD, Weiss M, Roberts MS 2000. An isolated in-situ rat head perfusion model for pharmacokinetic studies. Pharm Res 17(2):127-134.
24. Ouyang Y, Lien EJ 1984. Quantitative analysis of blood-testis barrier and pancreatic permeation as functions of physiochemical parameters. Acta Pharmaceutica Jugoslavica 34:201-205.
25. Hellman B, Sehlin J, Taljedal IB 1984. Glibenclamide is exceptional among hypoglycaemic sulphonylureas in accumulating progressively in beta-cell-rich pancreatic islets. Acta Endocrinol 105(3):385-390.
26. Marynissen G, Smets G, Kloppel G, Gerlache L, Malaisse WJ 1992. Internalization of glimepiride and glibenclamide in the pancreatic B-cell. Acta Diabetol 29:113-114.
27. Gylfe E, Hellman B, Sehlin J, Taljedal B 1984. Interaction of sulfonylurea with the pancreatic B-cell. Experientia 40(10):1126-1134.
28. Rowland M, Tozer TN. 1995. Clinical Pharmacokinetics: concepts and applications. ed., Baltimore: Williams and Wilkins.
29. Panten U, Burgfeld J, Goerke F, Rennicke M, Schwanstecher M, Wallasch A, Zunkler BJ, Lenzen S 1989. Control of Insulin-Secretion by Sulfonylureas, Meglitinide and Diazoxide in Relation to Their Binding to the Sulfonylurea Receptor in Pancreatic-Islets. Biochem Pharmacol 38(8):1217-1229.
30. Austin RP, Barton P, Cockroft SL, Wenlock MC, Riley RJ 2002. The influence of nonspecific microsomal binding on apparent intrinsic clearance, and its prediction from physicochemical properties. Drug Metab Dispos 30(12):1497-1503.
31. Worboys PD, Bradbury A, Houston JB 1997. Kinetics of drug metabolism in rat liver slices .3. Relationship between metabolic clearance and slice uptake rate. Drug Metab Dispos 25(4):460-467.
32. Joost HG, Holze S 1978. Uptake of Tolbutamide by Islets of Langerhans and Other Tissues. Experientia 34(10):1372-1373.
33. Banks WL, Stein ER 1965. Effect of Hydrazine on Protein Content of Various Tissues in Rat. Proc Soc Exp Biol Med 120(1):1-3.
34. Ladriere L, Malaisse Lagae F, Malaisse WJ 2000. Uptake of tritiated glibenclamide by endocrine and exocrine pancreas. Endocrine 12(3):329-332.

35. Balant L 1981. Clinical Pharmacokinetics of Sulphonylurea Hypoglycaemic Drugs. Clin Pharmacokinet 6:215-241.
36. Mudaliar S, Henry RR. 2005. The Oral Antidiabetic Agents. In Inzucchi S, editor The Diabetes Mellitus Manual, Sixth ed., New York: McGraw-Hill. p 167-201.
37. Kim KA, Park JY 2003. Inhibitory effect of glyburide on human cytochrome P450 isoforms in human liver microsomes. Drug Metab Dispos 31(9):1090-1092.
38. Kelder J, Grootenhuis PD, Bayada DM, Delbressine LP, Ploemen JP 1999. Polar molecular surface as a dominating determinant for oral absorption and brain penetration of drugs. Pharm Res 16(10):1514-1519.
39. Palm K, Luthman K, Ungell AL, Strandlund G, Beigi F, Lundahl P, Artursson P 1998. Evaluation of dynamic polar molecular surface area as predictor of drug absorption: comparison with other computational and experimental predictors. J Med Chem 41(27):5382-5392.
40. Abraham MH 2004. The factors that influence permeation across the blood-brain barrier. Eur J Med Chem 39(3):235-240.
41. Potts RO, Guy RH 1995. A Predictive Algorithm for Skin Permeability - the Effects of Molecular-Size and Hydrogen-Bond Activity. Pharm Res 12(11):1628-1633.
42. American Chemical Society. 2006. SciFinder Scholar. ed.
43. Hansch C. 1990. Comprehensive medicinal chemistry : the rational design, mechanistic study & therapeutic application of chemical compounds. ed., Oxford: Pergamon Press.

Tables

Table I. Physicochemical Properties of the Sulphonylureas Studied

Drug	Empirical Formula	Mol. Wt.	log P_{app} [a]	f_{uB} [b]	f_{uB} [c]	pK_a [d]
Tolbutamide	$C_{12}H_{18}N_2O_3S$	270.35	0.52	0.064 ± 0.001	0.069 ± 0.002	5.27
Chlorpropamide	$C_{10}H_{13}Cl\ N_2O_3S$	276.74	0.36	0.080 ± 0.008	0.105 ± 0.005	4.92
Gliclazide	$C_{15}H_{21}N_3O_3S$	323.42	-0.27	0.225 ± 0.046	0.181 ± 0.010	5.8
Glipizide	$C_{21}H_{27}N_5O_4S$	445.54	0.15	0.110 ± 0.010	0.081 ± 0.007	5.9
Glibenclamide	$C_{23}H_{28}ClN_3O_5S$	494.01	1.90	0.005 ± 0.0002	0.005 ± 0.0001	5.3
Glimepiride	$C_{24}H_{34}N_4O_5S$	490.63	1.08	0.011 ± 0.004	0.008 ± 0.002	5.3

[a]log P_{app} (octanol/water partition coefficient at pH 7.4) values from SciFinder Scholar [42].
[b]Unbound fraction (f_{uB}) of drug in 2% BSA MOPS buffer at pH 7.4, after incubation at 37°C for 30 min.

[c]Unbound fraction (f_{uB}) of drug in 2% BSA MOPS buffer, containing 15% (v/v) prewashed canine RBCs at pH 7.4, after incubation at 37°C for 30 min.
[d]pK_a (the negative logarithm of the ionization constant) values from [30,43].

Table II. Nonparametric and Parametric Moments for the Distribution of Reference Solutes and Sulphonylureas in the Perfused Rat Pancreas and Liver (mean ± SD).

	Pancreas perfusions (n=5)			Liver perfusions (n=4)	
Reference solute/Drug	MTT(s)[a]	CV[2b]	*E*[c]	MTT(s)	CV[2]
Albumin	8.9 ± 1.2	5.73 ± 2.85	n/a	8.5 ± 1.8	0.59 ± 0.08
Sucrose	16.9 ± 4.4	3.36 ± 1.55	n/a	10.3 ± 1.8	0.52 ± 0.05
Water	41.5 ± 10.5	3.38 ± 1.54	n/a	28.6 ± 5.8	0.71 ± 0.02
Tolbutamide	15.8 ± 7.2	6.43 ± 3.10	0.03 ± 0.09	21.7 ± 5.6	0.81 ± 0.13
Chlorpropamide	16.6 ± 10.3	6.43 ± 1.22	0.10 ± 0.07	20.2 ± 5.0	1.19 ± 0.19
Gliclazide	23.0 ± 7.6	6.78 ± 2.01	0.10 ± 0.07	68.0 ± 7.7	0.95 ± 0.16
Glipizide	15.3 ± 5.8	8.57 ± 1.33	0.43 ± 0.04	33.8 ± 9.2	2.34 ± 0.57
Glibenclamide	6.4 ± 2.9	5.82 ± 2.77	0.52 ± 0.04	6.2 ± 1.0	0.28 ± 0.15
Glimepiride	6.3 ± 1.5	6.83 ± 0.91	0.49 ± 0.12	7.3 ± 1.7	0.46 ± 0.22

[a] Mean transit time (corrected for catheter transit times).

[b] Normalized variance.
[c] Hepatic extraction ratio (E) = 1 – hepatic availability (F).

Table III. Model Derived Kinetic Parameters for Sulphonylureas in the Perfused Rat Pancreas and Liver (mean ± SD).

	Tolbutamide	Chlorpropamide	Gliclazide	Glipizide	Glibenclamide	Glimepiride
Pancreas Perfusions (n=5)						
k_{in} (s^{-1})[a]	0.099 ± 0.042	0.079 ± 0.038	0.14 ± 0.037	0.095 ± 0.022	0.048 ± 0.027	0.062 ± 0.041
k_{out} (s^{-1})[b]	0.023 ± 0.007	0.039 ± 0.016	0.036 ± 0.011	0.025 ± 0.007	0.0067 ± 0.0007	0.026 ± 0.026
k_{in}/ k_{out}	4.56 ± 2.38	2.44 ± 1.65	3.90 ± 0.56	4.17 ± 1.74	6.97 ± 3.39	4.56 ± 2.88
CL_{pT} ($ml \cdot min^{-1} \cdot g^{-1}$)[c]	0.89 ± 0.33	1.12 ± 0.31	1.53 ± 0.46	0.91 ± 0.26	0.42 ± 0.20	0.52 ± 0.29
PS ($ml \cdot min^{-1} \cdot g^{-1}$)[d]	15.2 ± 5.0	14.0 ± 3.8	6.7 ± 2.0	8.2 ± 2.3	63.9 ± 1.3	58.8 ± 15.3
Liver Perfusions (n=4)						
k_{in} (s^{-1})	0.19 ± 0.04	0.081 ± 0.033	0.22 ± 0.08	0.14 ± 0.03	0.12 ± 0.03	0.10 ± 0.04

k_{out} (s^{-1})	0.12 ± 0.03	0.053 ± 0.013	0.024 ± 0.003	0.0041 ± 0.0010	0.0018 ± 0.0014	0.0056 ± 0.0027
k_{in}/ k_{out}	1.73 ± 0.59	1.55 ± 0.59	9.48 ± 3.37	34.55 ± 11.11	56.04 ± 25.15	19.42 ± 7.57
k_e (ms^{-1})[e]	2.8 ± 5.6	2.1 ± 1.7	4.89 E-16 ± 2.84 E-19	1.3 ± 1.6	7.3 ± 9.2	21 ± 21
CL_{int} ($ml \cdot min^{-1} \cdot g^{-1}$)[f]	0.059 ± 0.117	0.055 ± 0.044	1.3 E-17 ± 8.2 E-18	0.044 ± 0.056	0.23 ± 0.31	0.65 ± 0.72
CL_{pT} ($ml \cdot min^{-1} \cdot g^{-1}$)	1.89 ± 0.53	1.30 ± 0.47	3.58 ± 1.08	2.18 ± 0.35	1.97 ± 0.44	1.63 ± 0.69
PS ($ml \cdot min^{-1} \cdot g^{-1}$)	23.6 ± 6.7	12.4 ± 4.5	19.9 ± 6.0	27.3 ± 4.4	393.1 ± 87.7	203.2 ± 86.4

[a] Permeation rate constant.
[b] Efflux rate constant.
[c] Permeation clearance.
[d] Permeability-surface area product.
[e] elimination rate constant.
[f] Intrinsic elimination clearance.

Table IV. Summary of Data used for Multiple Linear Regression.

Drug	Permeability Surface Area Product (ml/min^{-1}.g^{-1} liver)	Log P_{app}[e]	Number of Hydrogen bonding groups[f]	Polar Surface Area (10^{-10}m^2)[g]	Molecular Weight
Ampicillin[a]	0.9	-3.52	11	138	349.4
Atenolol[a]	0.38	-2.04	9	84.6	266.3
5-ethyl barbituric acid[a]	0.25	-0.35	not defined	not defined	156.2
5-methyl-5-ethyl barbituric acid[a]	37	-0.06	not defined	not defined	170.2
Diethylbarbituric acid[a]	53	0.56	7	75.3	184.2
5-nonyl-5-ethyl barbituric acid[a]	309	4.03	not defined	not defined	282.2
cefodizime[a]	0.51	-3.82	18	304	584.7
Diazepam[a]	137	2.8	3	32.7	284.8
Diclofenac[a]	220	1.5	5	49.3	318.1
Enalaprilat[a]	0.35	-5.84	10	107	348.3

Lidocaine[a]	180	1.64	4	32.3	234.2
4-methylumbelliferone[a]	66	1.58	4	46.5	176.2
Norepinephrine[a]	1.7	-2.29	9	86.7	169.2
Oxacillin[a]	0.52	-2.3	10	138	401.4
Salicylic acid[a]	4.6	-2.17	5	57.5	138.1
Warfarin[a]	62	0.22	5	63.6	308.3
p-Cresol[b]	152.2	1.19	2	20.2	108.1
p-Chlorophenol[b]	258.3	0.56	2	20.2	128.6
p-Iodophenol	500.7	1.17	2	20.2	220
p-propionamidophenol[b]	109.3	0.41	5	49.3	165.2
p-Cyanophenol[b]	112.1	1.05	3	44	119.1
p-Acetaminophenol[b]	80.16	0.1	not defined	not defined	151.2
p-Nitrophenol[b]	82.5	1.01	5	66.1	139.1
p-hydroxybenzoic acid[b]	9.14	-1.38	5	57.5	138.1
p-pentyloxyphenol[b]	165.7	0.44	not defined	not defined	180.2

p-heptyloxyphenol[b]	608.4	0.82	not defined	not defined	208.3
Phenol[b]	114	1.46	2	20.2	94.2
Antipyrine[c]	22.75	0.33	3	23.5	188.22
Prazosin[c]	28.06	1.88	11	107	383.41
Labetalol[c]	35.19	2.69	10	95.6	328.41
Propranolol[c]	55.33	3.1	5	41.5	259.34
Dilitiazem[c]	90.54	3.53	6	84.4	414.52
Tolbutamide[d]	23.58	0.52	7	83.7	270.35
Chlorpropamide[d]	12.37	0.36	7	83.7	276.74
Gliclazide[d]	19.9	-0.27	8	86.9	323.42
Glipizide[d]	27.27	0.15	12	139	445.54
Glibenclamide[d]	393.1	1.9	11	122	494.01
Glimepiride[d]	203.2	1.08	12	133	490.63

[a] data from [8].
[b] data from [4].
[c] data from [5].

[d] data from present study.
[e] octanol/water partition coefficient at pH 7.4.
[f] values from SciFinder Scholar [42].
[g] values from SciFinder Scholar [42].

Legends to Figures

Fig 1. Typical fit of outflow profile data of SUs (○ - A-tolbutamide, B-chlorpropamide, C-gliclazide, D-glipizide, E-glibenclamide, F-glimepiride) in the pancreas on a log-linear scale, together with albumin (●), used as a reference for the fitting. The lines indicate the fitted curves applying a physiologically based pharmacokinetic model (G). In the model, Q is the flow rate, k_{in} is the permeation rate constant and k_{out} is the efflux rate constant.

Fig 2. Typical fit of outflow profile data of SUs (○ - A-tolbutamide, B-chlorpropamide, C-gliclazide, D-glipizide, E-glibenclamide, F-glimepiride) in the liver on a log-linear scale, together with albumin (●), used as a reference for the fitting. The lines indicate the fitted curves applying a physiologically based pharmacokinetic model (G). In the model, Q is the flow rate, k_{in} is the permeation rate constant, k_{out} is the efflux rate constant and k_e is the elimination rate constant.

Fig 3. Regressions of mean transit time (MTT) and lipophilicity (log P_{app}) (A-pancreas, MTT = 18.72 – 7.74 log P_{app} (r^2 = 0.84; p<0.02); B-liver, MTT = 41.69 – 24.85 log P_{app} (r^2=0.69, p<0.05)), MTT and fraction unbound (f_{uB}) (C-pancreas, MTT = 7.77 + 74.33 f_{uB} (r^2 = 0.86, p < 0.01); D- liver, MTT = 1.98 + 323.64 f_{uB} (r^2 = 0.86, p<0.01)), normalized variance (CV^2) and log P_{app} in the liver (E, CV^2 = 1.03 – 0.40 log P_{app} (r^2 = 0.73, p=0.065)), CV^2 and log f_{uB} in the liver (F, CV^2 = 1.45 + 0.49 log f_{uB} (r^2 = 0.86, p<0.03)), hepatic extraction (E) and log P_{app} (G; E = 0.07 + 0.24 log P_{app} (r^2 = 0.71; p=0.067)) and E and log f_{uB} (H; E = -1.08 – 0.28 log f_{uB} (r^2 = 0.63; p=0.060)).

Fig 4. Regressions of permeation clearance (log CL_{pt}) and lipophilicity in the pancreas (log P_{app}) (A; log CL_{pt} = 0.08 – 0.26 log P_{app} (r^2 = 0.91, p<0.004)), log CL_{pt} and fraction unbound in the pancreas (log f_{uB}) (B; log CL_{pt} = 0.35 + 0.32 log f_{uB} (r^2 = 0.95, p<0.001)) and permeability surface area product (log PS) and log P_{app} in the

pancreas (C; log PS = 0.95 + 0.52 log P_{app} (r^2 = 0.89, p<0.01)) and log PS and log P_{app} in the liver (D; log PS = 1.24 + 0.71 log P_{app} (r^2 = 0.80, p<0.02)).

Fig 5. (A) Regression of permeability surface area product (log PS) and lipophilicity (log P_{app}) for combined data from previous studies (Chou et al., 1995; Mellick and Roberts, 1999; Hung et al., 2001) and the present work, in the liver (log PS = 0.37 log P_{app} + 1.36; r^2=0.62, n=38). The 95% confidence intervals are also shown. (B) Regression of log $PS_{predicted}$ and log $PS_{observed}$ where log $PS_{predicted}$ was estimated using only log P_{app} (log $PS_{predicted}$ = 0.63 log $PS_{observed}$ + 0.55; r^2=0.62, n=38) - closed circles and dotted line, log P_{app} and number of hydrogen bonding groups (log $PS_{predicted}$ = 0.76 log $PS_{observed}$ + 0.34; r^2=0.76, n=38) - open circle and dashed line, or log P_{app} and polar surface area (log $PS_{predicted}$ = 0.74 log $PS_{observed}$ + 0.39; r^2=0.75, n=38) - triangle and full line. Also shown are the 95% confidence intervals for the three models.

Figures

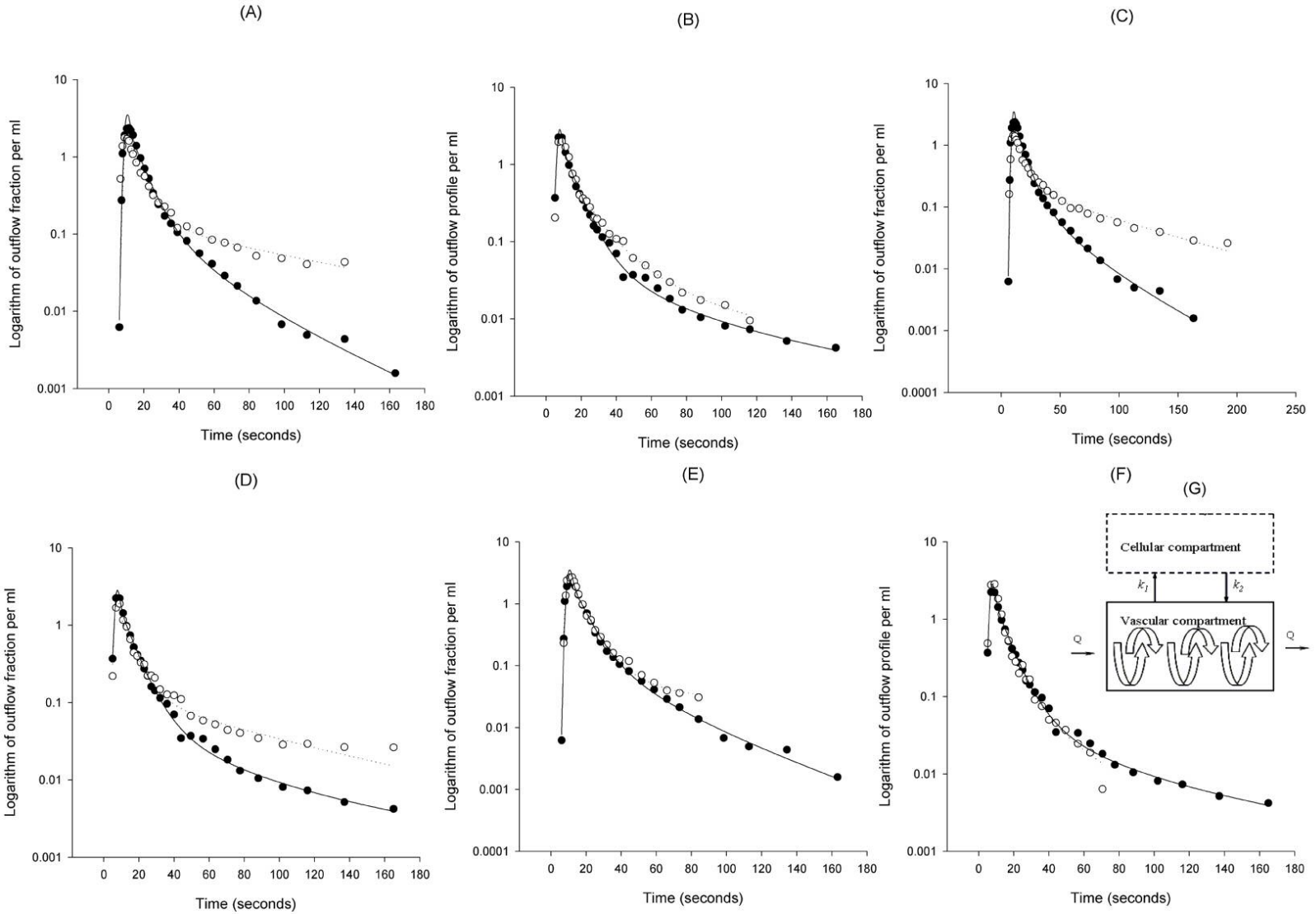
(A)
(B)
(C)
(D)
(E)
(F)
(G)
Logarithm of outflow fraction per ml
Logarithm of outflow profile per ml
Time (seconds)
Cellular compartment
Vascular compartment
k_1
k_2
Q

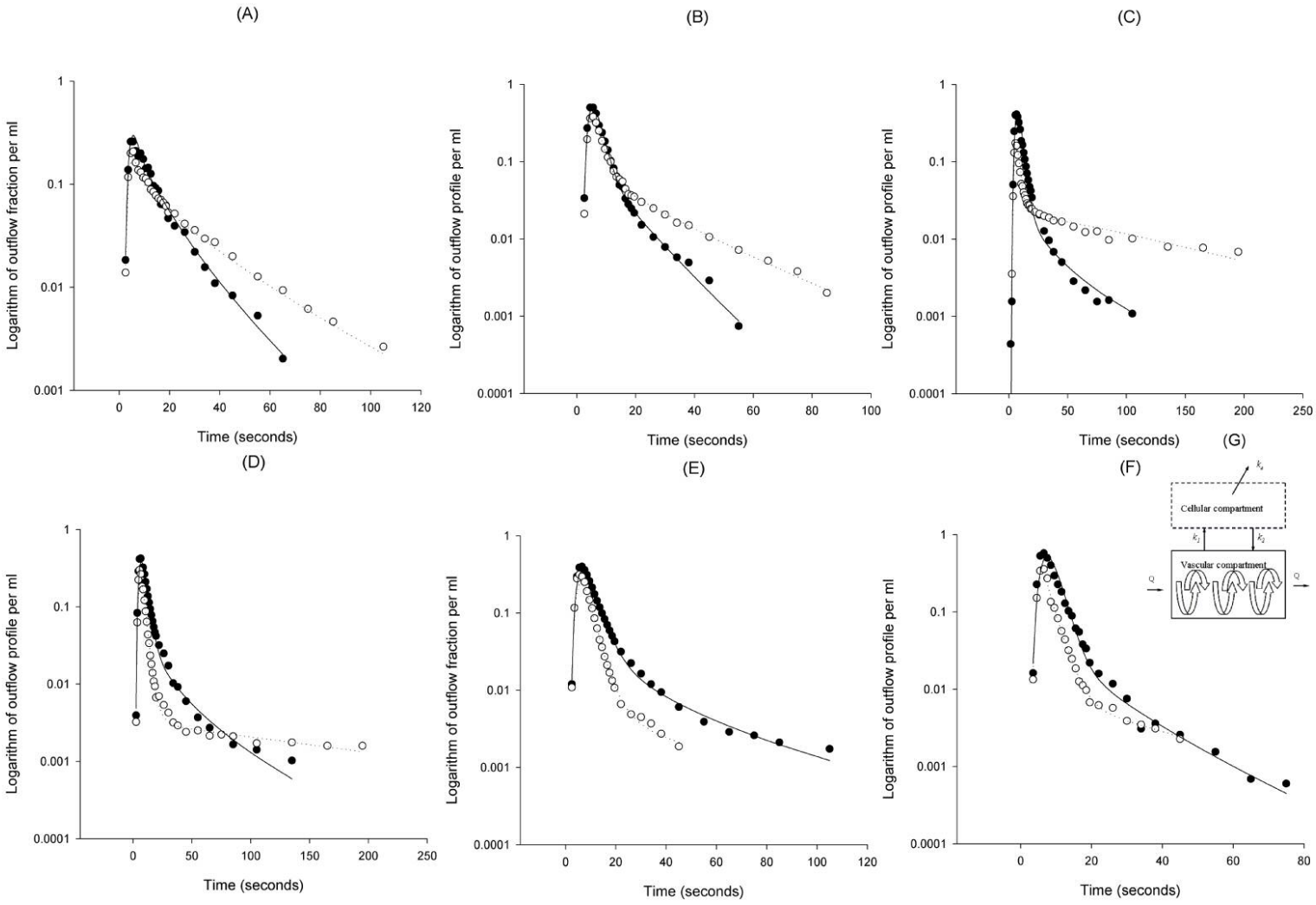
(A)
Logarithm of outflow fraction per ml
Time (seconds)
(B)
Logarithm of outflow profile per ml
Time (seconds)
(C)
Logarithm of outflow profile per ml
Time (seconds)
(D)
Logarithm of outflow profile per ml
Time (seconds)
(E)
Logarithm of outflow fraction per ml
Time (seconds)
(F)
Logarithm of outflow profile per ml
Time (seconds)
(G)
Cellular compartment
Vascular compartment

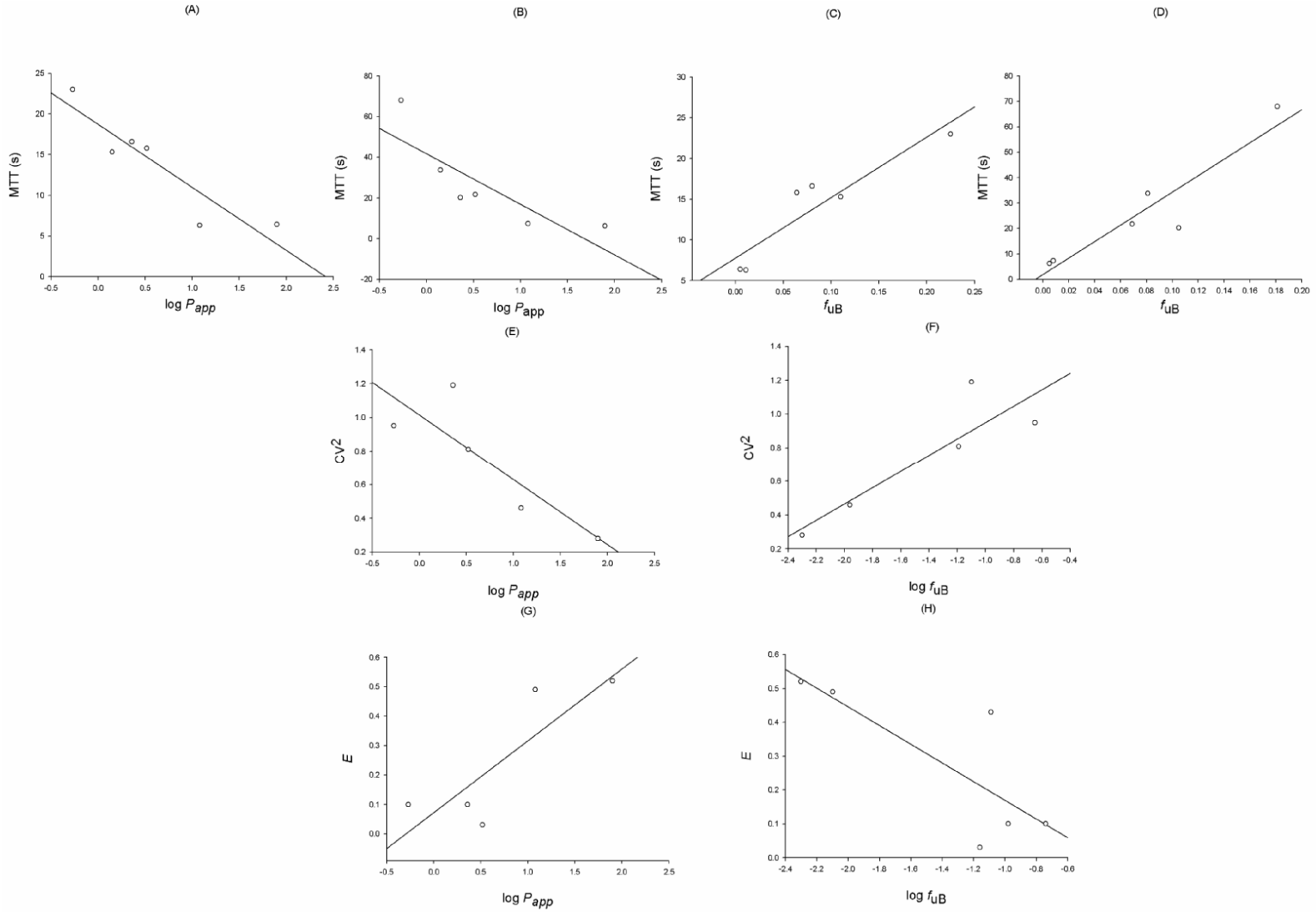
(A)
MTT (s)
log P_{app}
(B)
MTT (s)
log P_{app}
(C)
MTT (s)
f_{uB}
(D)
MTT (s)
f_{uB}
(E)
CV2
log P_{app}
(F)
CV2
log f_{uB}
(G)
E
log P_{app}
(H)
E
log f_{uB}

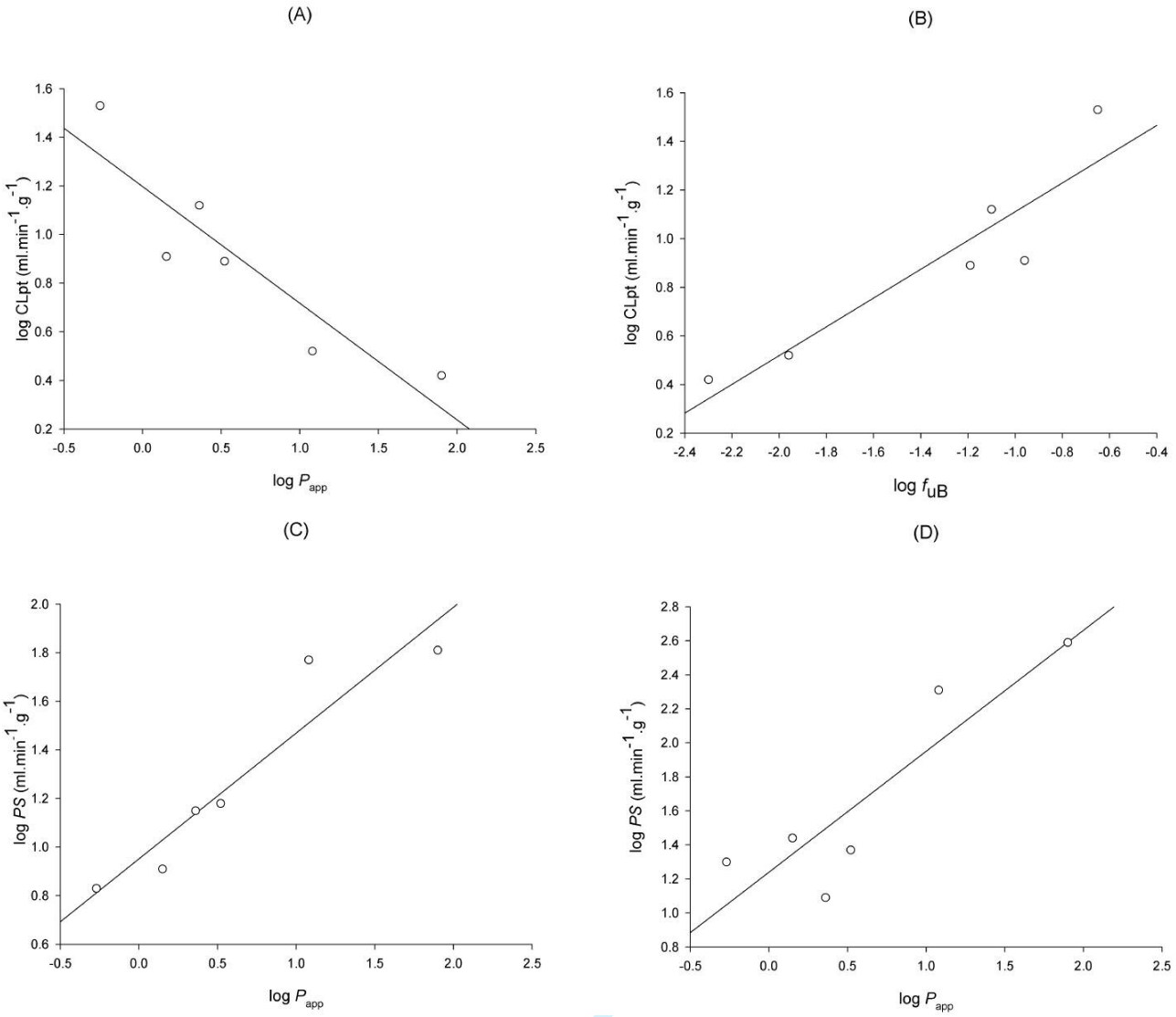
(A)
log CLpt (ml.min-1.g-1)
log Papp
(B)
log CLpt (ml.min-1.g-1)
log fuB
(C)
log PS (ml.min-1.g-1)
log Papp
(D)
log PS (ml.min-1.g-1)
log Papp

(A)

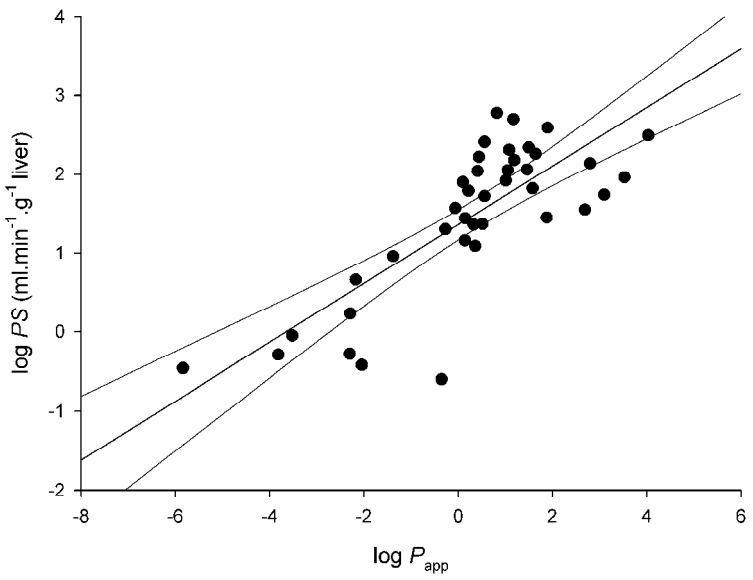
log PS (ml.min-1.g-1 liver)
log Papp

(B)

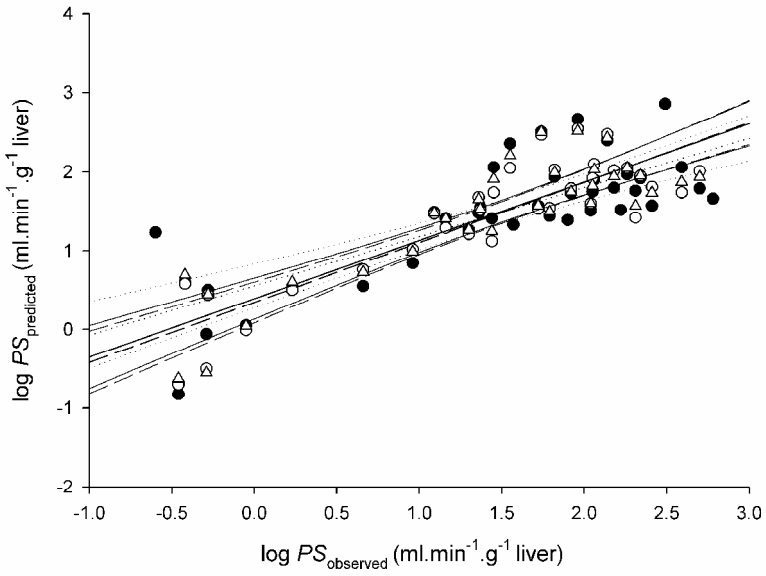
log PSpredicted (ml.min-1.g-1 liver)
log PSobserved (ml.min-1.g-1 liver)